Readout of TPC tracking chambers with GEMs and pixel chip

T. Kim, M. Freytsis, J. Button-Shafer, J. Kadyk, S.E. Vahsen, W.A. Wenzel

Lawrence Berkeley National Laboratory
Berkeley, California 94720, USA

Abstract

Two layers of GEMs and the ATLAS Pixel Chip, FEI3, have been combined and tested as a prototype for Time Projection Chamber (TPC) readout at the International Linear Collider (ILC). The double-layer GEM system amplifies charge with gain sufficient to detect all track ionization. The suitability of three gas mixtures for this application was investigated, and gain measurements are presented. A large sample of cosmic ray tracks was reconstructed in 3D by using the simultaneous timing and 2D spatial information from the pixel chip. The chip provides pixel charge measurement as well as timing. These results demonstrate that a double GEM and pixel combination, with a suitably modified pixel ASIC, could meet the stringent readout requirements of the ILC.

I. Introduction

One of the leading candidates for the central tracking chamber at the International Linear Collider (ILC) is the Time Projection Chamber (TPC) [1]. Although this technology was invented in 1976 and has been in use for many years, the registration of tracks has continued to depend upon the original use of wire chambers on the endcaps of the TPC to detect tracks. Signals induced on pads close to the anode wires are digitized and sent to the data acquisition system. The anode wires are interleaved with cathode wires in order to maintain uniform gain and electrostatic stability, and all wires need to be under tension. The large number of wires requires a strong support frame, usually a thick aluminum plate. Particles passing through this endcap plate, therefore, have a substantial probability of interaction, and detectors behind the endcap, such as calorimeters, suffer considerable degradation in performance.
The signal, produced primarily by the drift of positive ions away from the anode wires, has an intrinsically slow component. Moreover, this readout suffers an inherent error from deflection near the anode wire by the ExB effect [2]. The alternative avalanche devices discussed below do not have these deficiencies since their signals are from the electrons produced in the avalanche, which drift rapidly and nearly parallel to the B field.

The performance of an ILC detector as presently conceived requires considerable improvement over that of current detectors [3]. The generic performance required for charged particle tracking in the TPC is a point resolution in X-Y of 100 μm or less, with 200 or more 3D space points, and Z-resolution of 500 μm or less (Z being the central axis and beamline.) The required resolution in projected curvature, with inclusion of an intermediate tracker and vertex detector, is

$$\sigma(1/p_T) \sim 5 \times 10^{-5}\ \mathrm{GeV}^{-1}$$

at large momentum. To meet this requirement, the TPC alone must achieve nearly this value. This requires significant improvements in performance over that of previous TPC trackers. The uncertainty from diffusion is likely to be several hundred microns for an average drift distance of about one meter in the 3 - 4 T magnetic field of current designs. These resolutions from the track readout should be small compared with that value.

These resolution requirements can be achieved using gas avalanche devices such as the Gas Electron Multiplier (GEM) [4] or Micromegas [5], followed by an integrated pixel chip, or Application Specific Integrated Circuit (ASIC), with small and closely spaced pixels. To aid in particle identification, track ionization can be determined either by charge measurement or by cluster counting by the chip. The final detector design has not yet been chosen, but most candidates have the TPC as the central tracking device. The general concepts underlying the TPC operation are not very different among these candidates, which are sufficiently similar for the studies described here.

Our test system is composed of a two-stage (two-GEM) electron avalanche multiplier, followed by the FEI3 ATLAS front-end pixel chip [6]. We detect and record cosmic ray (CR) tracks as a source of tracks for our studies. As used here, this term includes tracks induced by CRs, such as delta rays produced by the CR and Compton recoil electrons from low-energy photons in a CR-induced electron shower. Drifting electrons arising from the ionization trail of primary particles are multiplied by electron avalanching in the double GEM, and the resulting charge is collected by the FEI3. The double GEM is capable of a total avalanche gain > 40,000, but in these investigations a smaller gain is used, partly to reduce the risk of discharge or sparking, which could easily damage the chip. The FEI3 collects the charge on 50-by-400-μm pixels. The charge is digitized and timed on the chip and read out by associated electronics. A post-processing step covered each pixel with a conductor (aluminum or gold) to maintain uniformity of the electric field and to avoid charge accumulation on the pixel surface, which is otherwise an insulator (silicon). The FEI3 has a self-trigger feature, which we use to trigger on cosmic rays.

II. Description of apparatus and techniques

A. Double GEM and pixel chip test system

1. Geometry of test system

The avalanche multipliers used for the measurements and results presented here are GEMs obtained from the CERN store with the following "standard" design [7]:

Active area	5 cm x 5 cm
Pitch (center-to-center hole spacing)	140 μm
Physical area, including frame:	7 cm x 7 cm
Thickness of GEM insulating layer (Kapton):	50 μm
Thickness of each GEM electrode (copper):	5 μm
Thickness of frame:	1.3 mm

Figure 1(a) shows the geometry and the important dimensions of the two-GEM plus FEI3 test configuration, and Fig. 1(b) is a view of a GEM foil and frame.

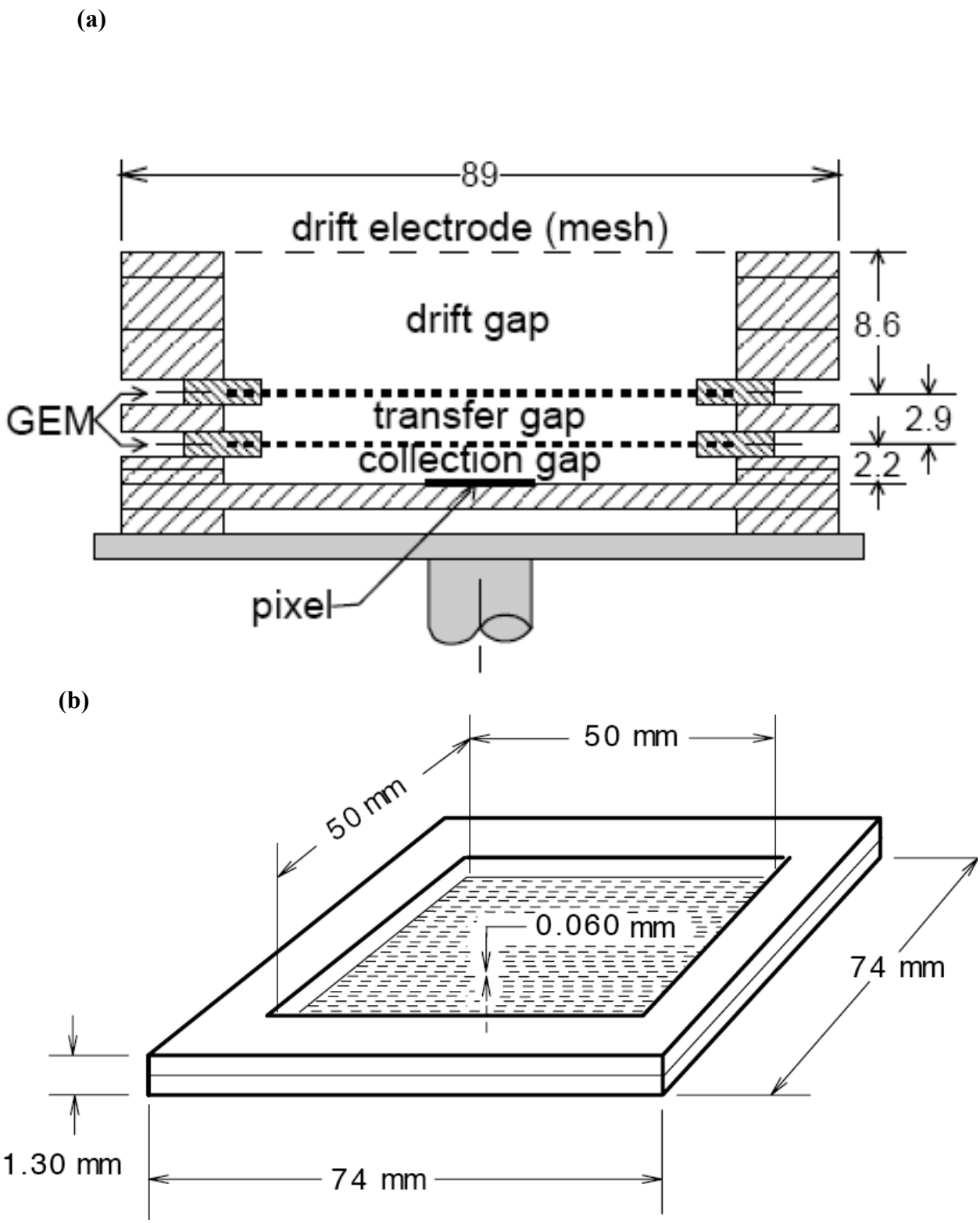

Fig. 1. (a) The detector assembly is shown in cross section and is rectangular in plan view. The entire detector package, supported by a steel plate, is secured at the corners by four vertical plastic bolts (not shown). The insulating spacers are of Lucite or G10. Dimensions are in millimeters. (b) A single GEM foil is shown mounted in a G-10 frame. The foil is of a standard CERN design, having 50-μm thick Kapton insulator between 5-μm thick copper sheets on upper and lower surfaces, and 140-mm pitch between avalanche holes [7].

The test system consists of (top to bottom): (1) drift electrode (cathode); (2) drift gap of 8.6 mm, in which charged tracks produce primary ionization; (3) the upper GEM1, separated by (4) a 2.9-mm transfer gap from the lower (5) GEM2; (6) the 2.2-mm collection gap (or induction gap) and (7) the pixel chip, FEI3, and the surrounding collection electrode or pad. The collection electrode is a single thin square copper pad, about 9 cm on each side; the pixel chip is mounted in a small hole in the center, insulated from the pad and closely fitting the chip transverse dimensions (see Fig. 2).

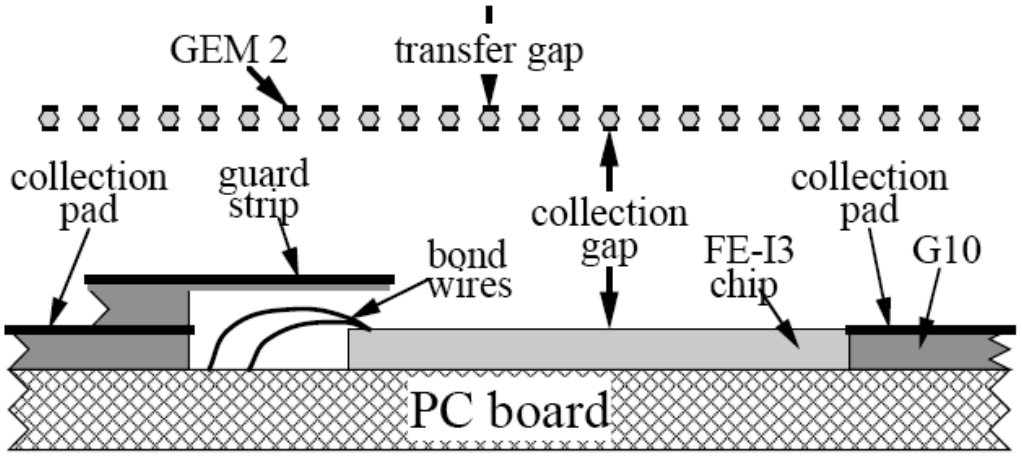

Fig. 2. A detailed view (not to scale) of the FEI3 pixel chip mounted on the custom PC board, and surrounded by the collection pad. The bond wires carry the pixel signals to the signal processing electronics on the underneath side of the PC board. The guard strip shields the bond wires from the field to prevent possible avalanching.

The chip is mounted with its top surface coplanar with that of the collection pad to maintain field uniformity. Charge from GEM2 is collected either on the chip or on the surrounding collection pad, both at ground potential. From a collimated ^{55}Fe source about 2 cm off-center, charge was collected on the pad, and the performance and gain of the double-GEM system was monitored with an oscilloscope and a pulse-height analyzer [8].

The chip is glued with conducting epoxy cement to a specially designed PC board, with wire bonding to lines connecting to readout components located on the opposite side. A small guard strip just above the bond wires is electrically connected to the collection pad to prevent any unwanted avalanching or other electrical problems associated with the relatively large collection field (~3kV/cm) in the vicinity of the wires.

The GEMs, pixel chip and readout are firmly secured together by four plastic mounting screws (not shown) through the corners of the square configuration of GEMs and plastic spacers. This package was mounted inside a cylindrical stainless steel test vessel (TV) with approximate inside dimensions 25 cm diameter by 10 cm height. The removable cover plate has a thin (0.25 mm) Mylar window for testing with a ^{55}Fe X-ray source. Wall penetrations of the TV are: (1) high voltage feedthrough connectors welded into the TV wall; (2) low-voltage and signal leads through a 50-pin feedthrough connector glued into a wall penetration; and (3) steel tubing for gas inlet and outflow welded into the TV wall. The gas flow rate was typically 30 cm^3/min, monitored at both the entrance and exit of the vessel to ensure reliable flow and absence of leaks. Periodic leak checks were made at a high level of sensitivity.

2. Gas mixtures tested

The gases used in these investigations included: (1) argon/carbon dioxide (70/30), a very good operating gas for GEMs; (2) argon/isobutane (95/5); and (3) argon/methane/carbon dioxide (93/5/2). Individual GEMs were tested at CERN and by us before combining into the double-layer configuration. These gave reliable maximum avalanche gains of about 300, without sparking, using the gas mixture: Ar/CO_2 (70/30). At larger gains, some sparking was experienced, but always without damage to the GEMs or any other test components. Although (1) is an excellent operating gas mixture for GEMs, for stability and aging, the mixtures (2) and (3) have larger electron drift velocities at modest drift fields more appropriate for use in the TPC, for fast electron drifts and good spatial resolution [9].

3. Power supply and electronics

A two-channel, high-voltage (HV) power supply [10] shown schematically in Fig. 3 supplied the voltage for the drift electrode on one channel, and the power for the GEMs on the second channel.

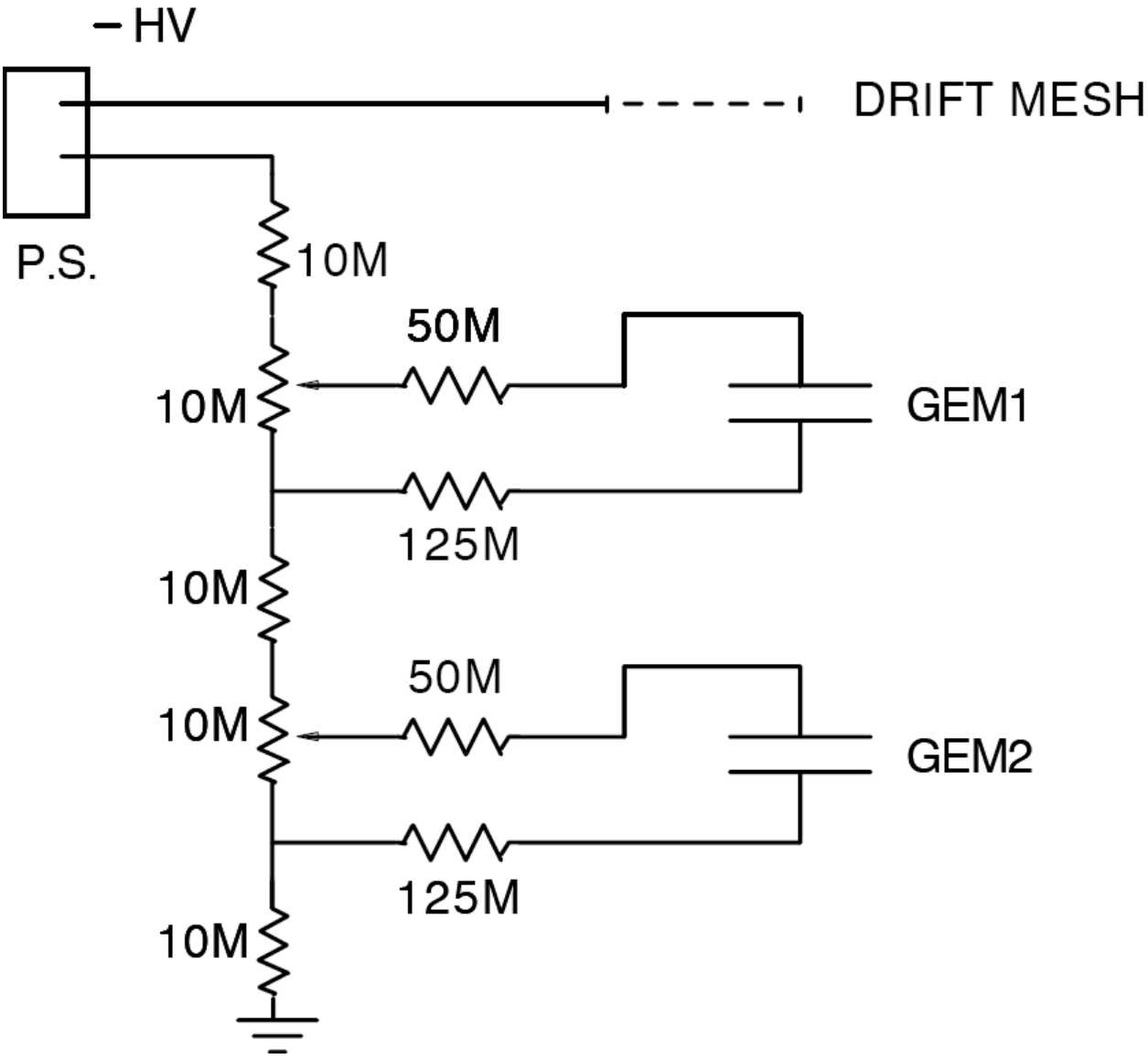

Fig. 3. The power-supply system for the drift electrode and the two GEMs. Voltages across the GEMs were set using the potentiometers, as indicated.

A resistor chain with two potentiometers set the GEM voltages. In this way the GEM gains could be varied individually, but the resulting drift and transfer gap fields therefore depended somewhat, but not sensitively, upon the GEM voltage settings. There are two protective resistances, of 50 MW and 125 MW in series with each GEM.

The active elements of the amplifier system are (Fig. 4): a charge-sensitive preamplifier [11] with 20 ns rise time, 1.03 ms fall time and a transfer response of 3.6 V/pC, and a TranLamp amplifier-shaper [12], with settings of 2 μs for both the integration and differentiation times, and a response of 21 mV/pC.

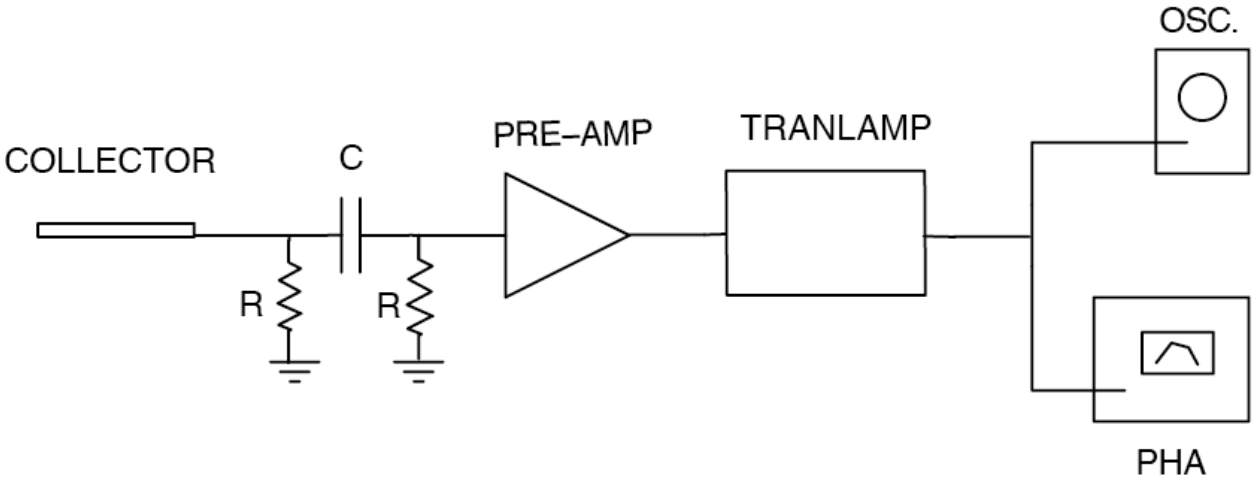

Fig. 4. A schematic diagram is shown of the electronic components for the amplification of the signal from the collection pad. The resistor-capacitor network completes the DC circuits for the GEM system and for the preamplifier input. The integration and differentiation time constants of the TranLamp are set to 2.0 μsec [12]. Values of components shown are R=1 MΩ and C=0.001 μF.

Incorporated in the preamplifier is a 1.0 pF test input capacitor used for gain calibration. Just ahead of the preamplifier is a resistor-capacitor network that (1) completes the DC circuit for the GEM test system, and (2) provides the DC return for the input to the preamplifier. The time constant of this circuit is long enough not to affect the measurements under study. A calibration of the entire system response, including the collection pad and its associated capacitance, is 51 V/pC.

4. Spectra measurements and gain calibrations

Spectra for the GEM system used a collimated ^{55}Fe source of about 1 mCi activity above the drift gap, but translated about 2 cm off center, so that essentially all the charge from the converted X-ray was collected on the copper collection pad. The spectra were recorded on a pulse height analyzer [8], which was calibrated using a precision pulse generator. An example spectrum is shown in Fig. 5. Typically, the relative width of the main peak is 24% FWHM.

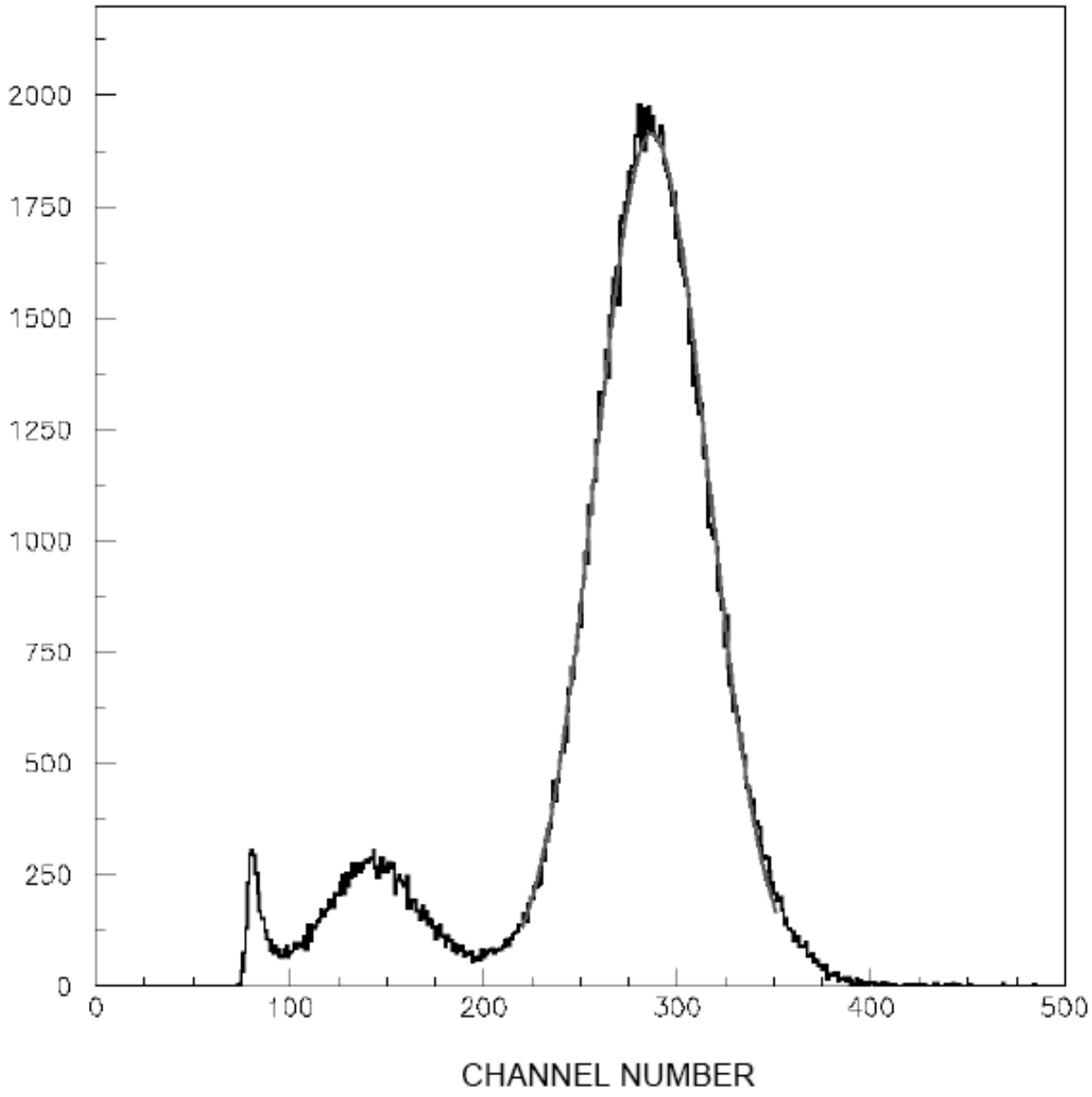

Fig. 5. A typical spectrum from the double-GEM detector in response to incident 5.9-keV X-rays from an ^{55}Fe source. The escape peak, at approximately half the energy of the main peak, is well resolved. The width of the main peak is 24% FWHM.

The avalanche gain was determined from these spectra using the calibrated system response and assuming the primary ionization from the 5.9-keV X-ray conversion events to be 220 electron-ion pairs. The measured gain is, of course, an "effective" gain, including whatever loss of electrons occurs in the charge flow through the two GEMs to the collection pad. For large gains and signal amplitudes, a capacitor was placed in parallel with the collection pad, reducing the input signal to the preamplifier, to keep it within its operating range. The new calibration was determined by measuring the same spectrum both with and without the added capacitance, keeping both measurements within the operating range of the amplifier system.

Measurements of avalanche gain vs. GEM voltages will be presented in section III.

B. The FEI3 ATLAS pixel front-end chip

1. Introduction

The FEI3 [6] is an integrated circuit chip using 0.25-µm CMOS technology that was designed, produced, and tested by the ATLAS collaboration for use in the ATLAS pixel detector [13]. The chip, having an active area of 7.2 mm x 10.8 mm, contains about 3.5 million transistors and 2880 pixels of dimensions 50-by-400 µm arranged into 18 columns by 160 rows. A microphotograph of the surface of the chip is shown in Fig. 6.

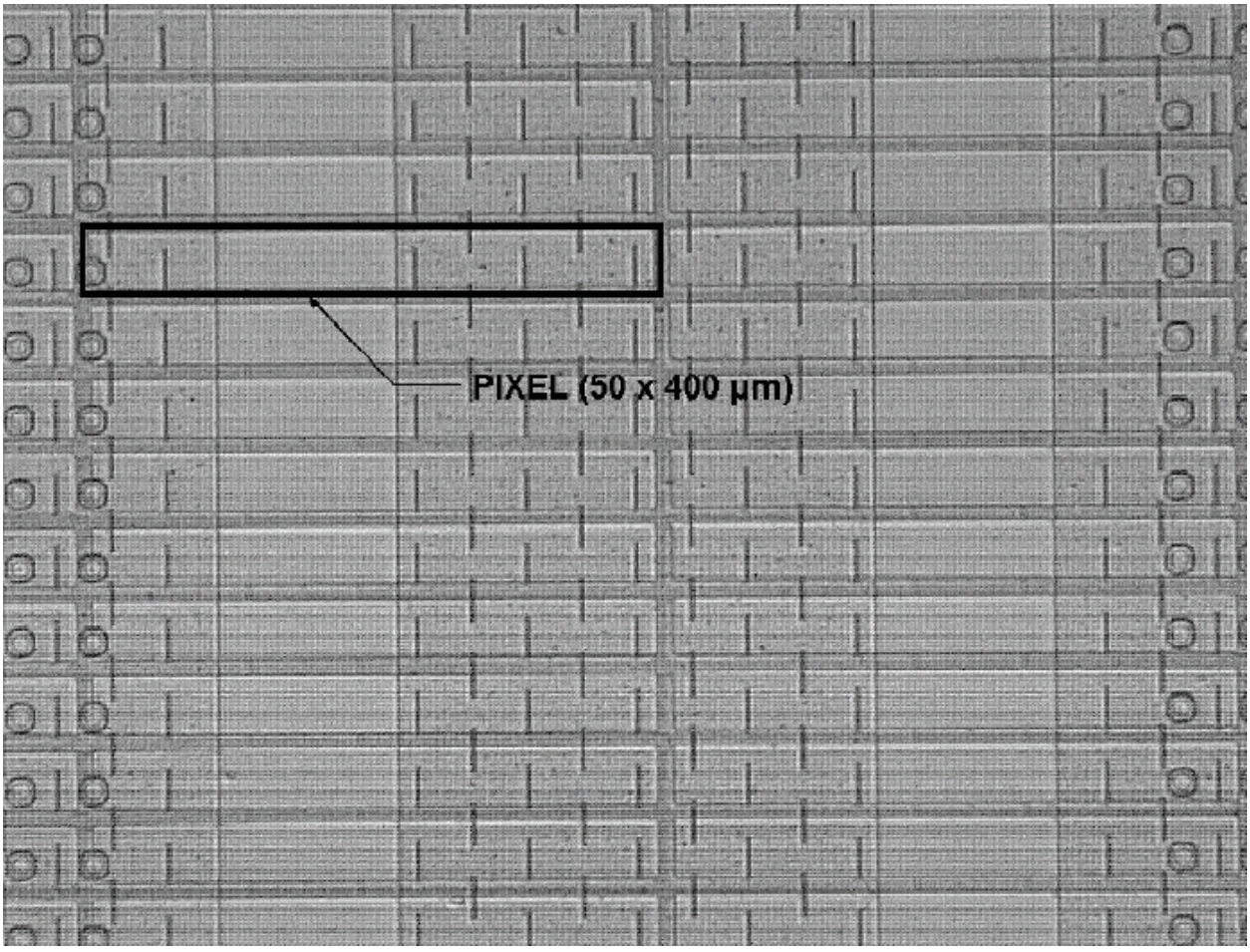

Fig. 6. Microphotograph of the surface of the ATLAS FEI3 chip after deposition of gold. One of the 50 x 400-micron cells is outlined. The entire chip, containing 2880 pixel cells, is 7.2 mm by 10.8 mm in surface dimensions and is 700 microns in thickness.

The rectangular pixels, gold-plated in this case, are clearly evident, as is the electrical connection to chip circuitry. The thickness of the chip used in our tests is about 700 µm, but our chip could be thinned to 190 µm (0.2 % radiation length), as was done with the ATLAS chip, or even thinner. The design is radiation-hard and has been demonstrated to operate after a 100 MRad irradiation dose.

The FEI3 is optimized to meet ATLAS and LHC requirements for spatial resolution, occupancy, timing, buffering and power. The pixel size and the on-chip digital buffer were chosen to record

up to 5x107 hits/cm2/sec with efficiency greater than 99% and approximately 14 μm spatial resolution in the precision direction. Hits are buffered for up to 3.2 μs, and time bins of 25 ns distinguish LHC bunch crossings. The chip has a self-triggering capability and can read out hits from up to 16 subsequent time bins after a trigger. Most of these design choices would change for the intended TPC readout.

In ATLAS, FEI3 chips collect and digitize charge pulses from primary particles traversing pixilated silicon sensors. The sensor pixels are connected to the pixels on the FEI3 via bump bonds. In our case there is no silicon sensor; the charge signal is from electron avalanche multiplication in the double GEM. The amplified charge then drifts directly onto the pixel surface. Since the surface of the normal FEI3 chip consists almost entirely of insulator (silicon nitride, except for 12 μm bonding "bump" openings), we have post-processed the chip to cover each pixel with a thin rectangle of aluminum or gold, connected to the original bump-bond opening. This covering collects the charge and prevents charge accumulation on insulating surfaces, while maintaining insulating boundaries between pixels and a uniform electric field in the collection gap. Both aluminum and gold were used in the post-processing step, to check whether potential oxidation of aluminum might be a concern. (It was not.)

Some of the 50-by-400-μm pixel cells are visible in Fig. 6, along with the electrical connection to the surface conductor. The performance of the pixel chip and uniformity of response was verified by pulse-height studies with the ^{55}Fe source centered directly above the chip, as well as by charge injection into each pixel using a test routine of data-acquisition program.

2. Functionality of each pixel cell

Each pixel channel consists of an integrating, charge-sensitive amplifier followed by a discriminator and digital readout. Each pixel channel has a digital control for adjusting the threshold, return-to-zero slope of the amplifier's output voltage, separate enable/disable for analogue and digital circuits, and enable/disable for inclusion in the trigger. The pixel also contains an internal injection circuitry, which we use for calibration. When a pixel's amplifier output rises above threshold, a hit is generated and buffered digitally on-chip until a trigger occurs. The data retained for each hit are the spatial coordinates, arrival time and the time over threshold (TOT). The TOT allows a measurement of the charge collected. Both arrival time and TOT are stored on the chip in units of clock cycles, or 1/f, where f is the clock frequency. During nominal operation in ATLAS, the FEI3 chip is clocked at 40 MHz, so that the arrival time and TOT are measured in 25-ns units.

3. Calibration

We use the FEI3's internal injection capability and digital controls to calibrate each pixel to a threshold near 1800 electrons, and TOT scale of approximately 700 electrons per clock cycle. Both numbers are uncertain by 20-30%, as the internal-calibration charge scale is known to have a systematic uncertainty of that magnitude. Using internal injection tests, we determine the noise level to be 121 ± 9 electrons. With this threshold setting, we achieve stable operation of the system, with only 2 or 3 noisy pixels, out of 2880. Without masking noisy pixels, the measured rate of noise hits was 0.2/min, and after masking these, there were no noise hits after several hours.

4. Connectivity

Our power, control, and data-acquisition schemes for the FEI3 are similar to what has been used during development and production testing of the FEI3 in ATLAS. We read out the FEI3 using a combination of custom data-acquisition electronics and a generic PCB-to-VME interface, controlled by the data-acquisition program "TurboDAQ" [14]. However, we designed a new PC board for the upstream end of the DAQ chain. While providing the same power, control and

readout functionality as the original ATLAS board, it mounts only the chip on one side. All the other chips and power connections are mounted on the other side of the board, and do not interfere with the GEM system. (see Fig. 2.)

5. Trigger

The FEI3 generates a fast digital-OR signal of all trigger-enabled pixels, which we use to self-trigger the FEI3 on cosmic ray tracks. We read out hits which arrive in the 16 time bins after the trigger, corresponding to 400 ns at the nominal ATLAS clock frequency f = 40 MHz. With small drift fields, f is decreased to 20 MHz or 10 MHz, increasing the duration of each time bin, as longer drift times may require more than 400 ns to record all charges produced in the 8.6-mm drift gap. For example, the drift velocity in the Ar/CO_2 gas at a drift field of 500 V/cm is only about 12 μm/ns, requiring 720 ns maximum drift time. At 20 MHz the entire drift gap is measurable.

For most studies we used a pixel threshold of about 1800 electrons, well above the noise level with the GEM gain set to zero. When studying the cosmic-ray trigger rate versus avalanche gain, however, we increased the pixel threshold to 5000 electrons, since some increase in noise was observed at large gains. With this setting we observed a plateau in the trigger rate, suggesting that single electrons as well as electron clusters were detected in the cosmic ray tracks. This will be discussed further in section III.D.

III. Measurements and results

A. Operating voltages

The double GEM system has operated reliably using the Ar/CO_2 gas mixture with maximum avalanche gains somewhat above 40,000. At larger gains, some sparking was observed in the GEMs, but without damage to the GEMs or the chip. Since the pixel chip is expected to be vulnerable to sparking of a GEM, or discharge of any kind, the gain on GEM2, closer to the chip, usually was kept smaller than that of GEM1. Typical electrode voltages in this "standard" configuration, corresponding to a gain of approximately 21,000, are (absolute values):

V(Drift Electrode)	= 2800V	
		E(drift) = 0.58 kV/cm
V(top GEM1)	= 2300V	
		VG1 = 500 V
V(bottom GEM1)	= 1800V	
		E(transfer) = 2.8 kV/cm
V(top GEM2)	= 1000V	
		VG2 = 400 V
V(bottom GEM2)	= 600V	
		E(collection) = 2.7 kV/cm
V(pixel chip)	= 0V	

B. Measurements of avalanche gain and energy resolution

For measurements of pulse-height spectra and avalanche gain, a collimated ^{55}Fe source is placed on the thin Mylar window above the drift electrode and about 2 cm transverse to the central axis, so that the avalanche charge is collected on the collection pad and not on the chip. Some charge is unavoidably lost to the electrodes of both GEMs, so that the gains measured in this manner are "effective" avalanche gains. The gains were measured over a broad range of voltages. Figure 7 shows the effective gain versus the GEM2 voltage (VG2) for several values of the voltage across

GEM1 (VG1), for the three gas mixtures. Figure 7(a) shows the gain for the Ar/CO_2 (70/30) gas mixture. Figure 7(b) and Fig. 7(c) present gain plots for the gas mixtures Ar/isobutane (95/5) and $Ar/CO_2/CH_4$ (93/5/2).

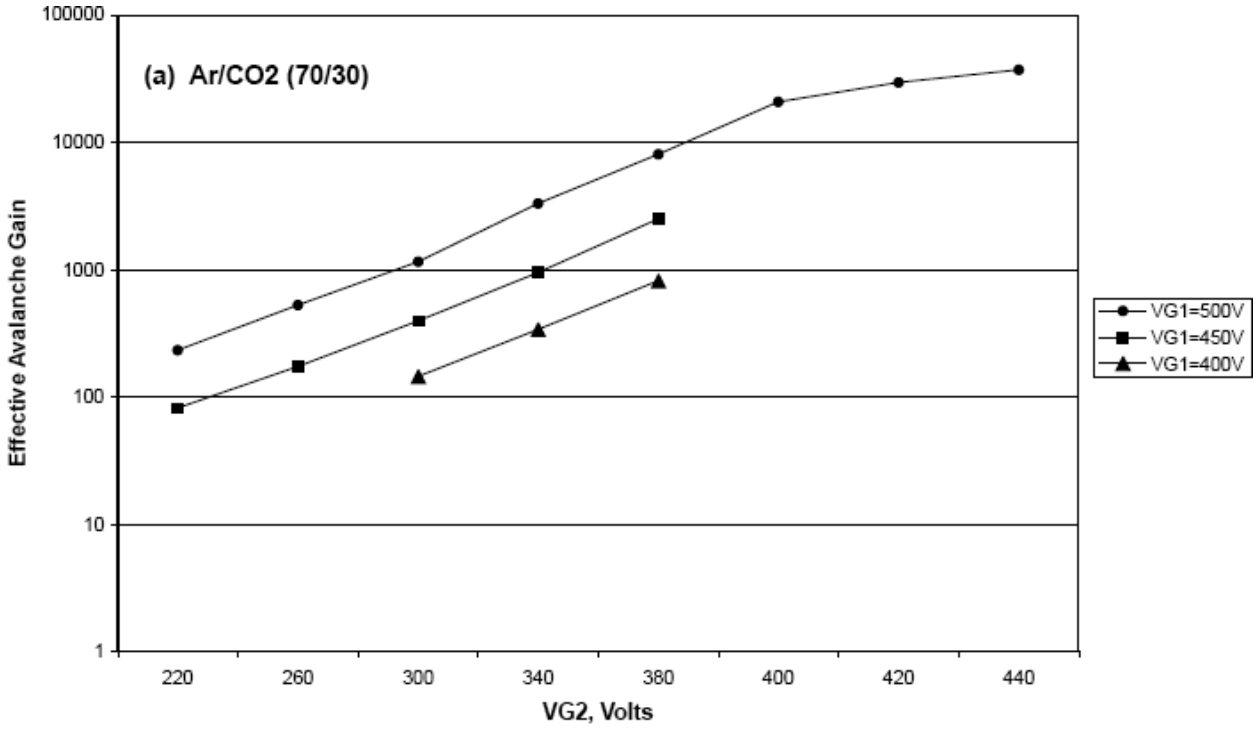

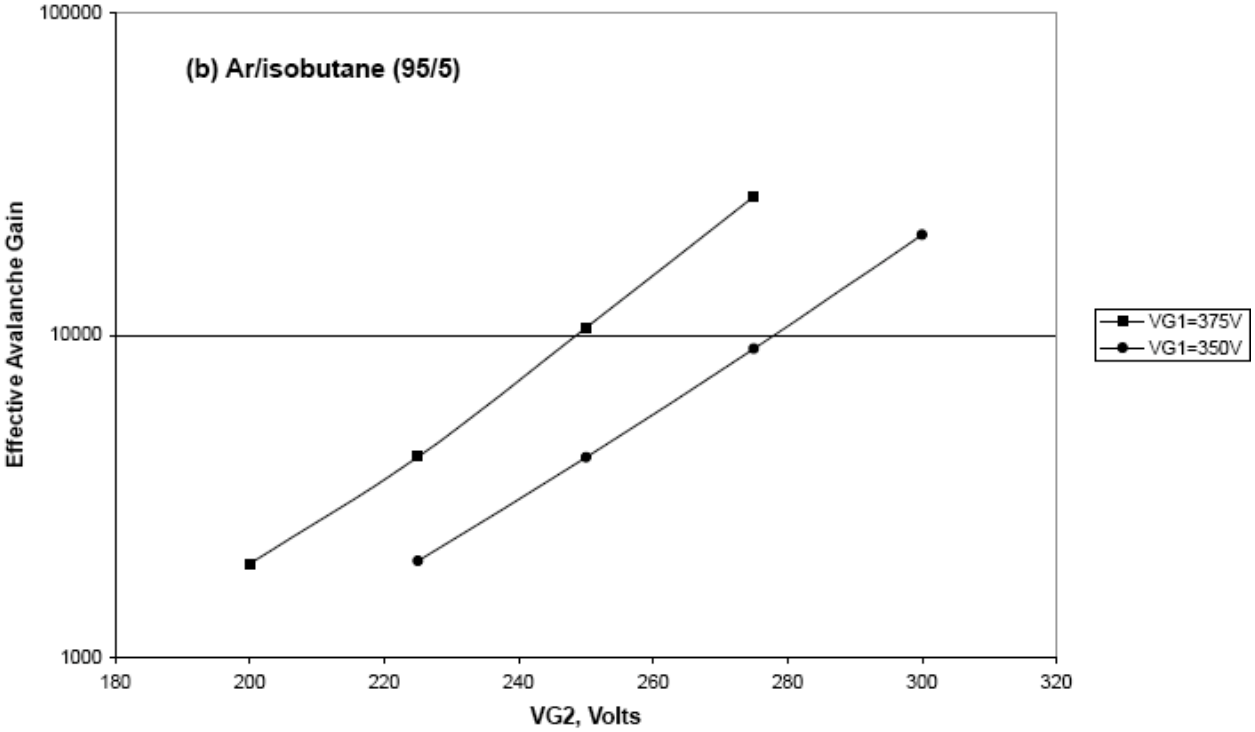

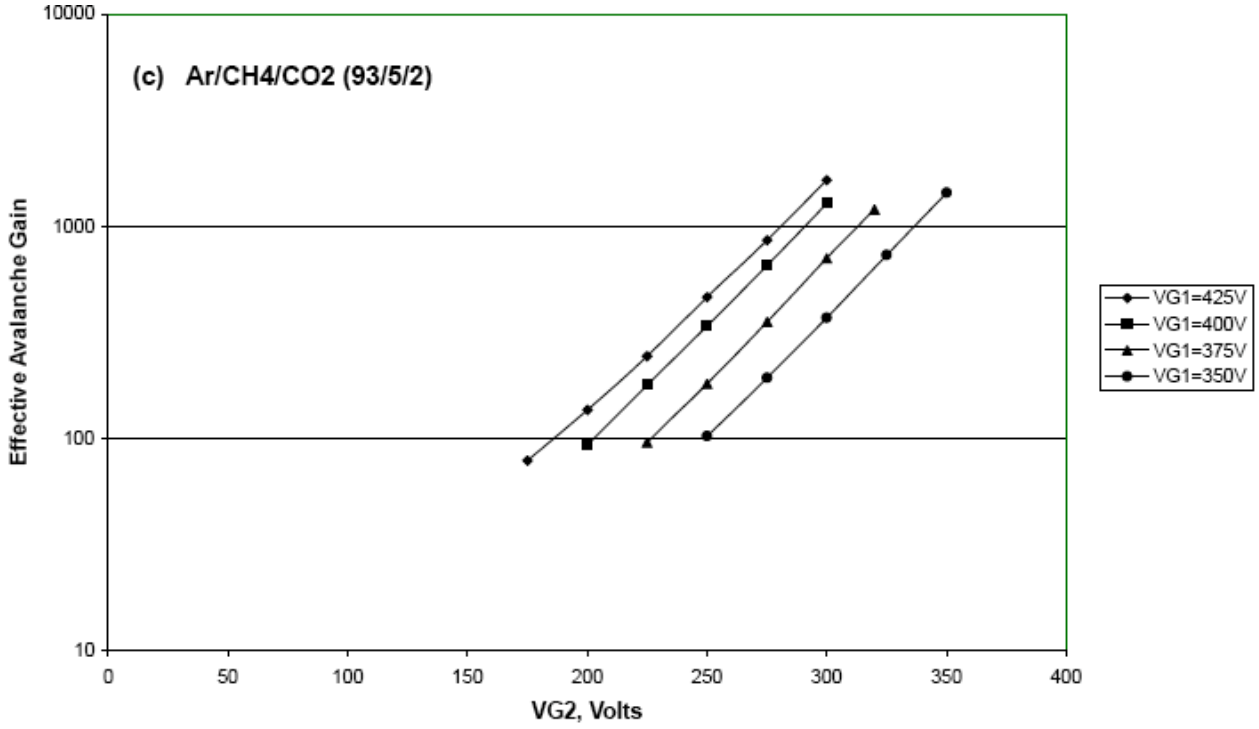

Fig. 7. Effective avalanche gain vs. GEM1 and GEM2 voltages, VG1 and VG2, respectively, are plotted for the three gas mixtures tested: (a) argon/carbon dioxide (70/30), (b) argon/isobutane (95/5) and (c) argon/methane/carbon dioxide (93/5/2). The gains are shown on logarithmic plots to show clearly in both the low and high gain regions. The plots extend to the largest gains observed until either the ^{55}Fe spectrum deteriorated or there was physical damage to a component (see text).

The track ionization can be determined either from the charge deposited on each pixel, or from counting the number of clusters or hits per unit length along the track. At this level of precision, the measurement of relative track ionization is not limited by that of individual pixels, but by the number of samples along the track. For a track of 10-cm length, the estimated average number of cluster hits for a minimum ionizing particle is about 300, and the relative ionization is expected to be known to a precision of ≤10%.

C. Experience with different gas mixtures

Although the Ar/CO_2 (70/30) gas mixture (1) performs reliably with large avalanche gains, the drift velocity is relatively small except at large drift field strengths [9]. This is somewhat disadvantageous for experiments that expect large event rates and require very good spatial resolution, as will be the case at the ILC. Larger drift velocities can be obtained with either of the other two gases, (2) or (3) [9]. However, there were two instances of damage to our GEMs, and also to the pixel chip while using the isobutane mixture. We believe it is likely that aging processes were responsible for the GEM damage, because these problems occurred soon after testing of this gas began, and no such damage was experienced during months of testing with the Ar/CO_2 mixture (1), even though some sparking had occurred. Moreover, one failure occurred using (2) without an audible spark, suggesting that a polymer fiber may have shorted the damaged GEM. The GEMs and the chip were replaced to continue tests with mixture (1), giving results quite similar to those of the earlier tests with mixture (1). Later, we began tests using gas (3).

The gas mixture (3) behaved well at small avalanche gains, but we experienced problems when the double-GEM gain was much above 1000. The spectra showed evidence of feedback in the

avalanches, possibly from ions or photons, manifested as major peaks in the spectra, both below and above the two normal ^{55}Fe peaks. Insufficient quenching appears to be the cause of the subsidiary peaks and the inability to achieve the larger gains obtained with the other two gas mixtures. When the gain was increased to nearly 11,000, damage from sparking occurred. Since our pixel chip requires thresholds of 1800 electrons or larger, this operating gas may not be adequate for use with this chip. However, future applications for TPC readout may use ASIC chips with smaller intrinsic noise, due to smaller pixel area, permitting lower thresholds and avalanche gains [15].

Similar studies with gas mixtures (2) and (3) have been reported, but not with an ASIC readout [16].

D. Cosmic ray measurements

Figure 8 shows the cosmic ray (CR) counting rate vs. the effective avalanche gain of the double GEM.

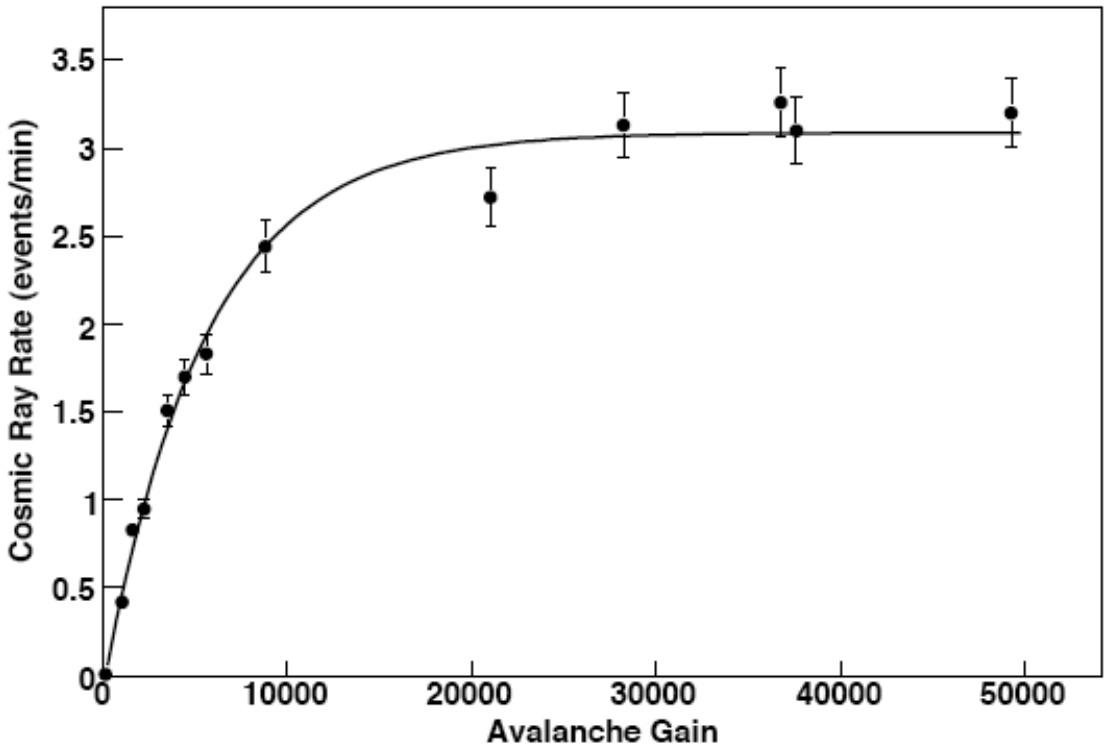

Fig. 8. Cosmic ray counting rate vs. the effective avalanche gain of the double GEM. The threshold of the FEI3 was 5000 electrons. The plateau level of about 3 events per minute is consistent with the expected rate when the geometry is taken into account. The increase of the curve to the plateau value occurs at a gain that is consistent with the trigger threshold of 5000 electrons and the gain of the double GEM system. The plateau value is consistent with single electrons as well as electron clusters being detected from the cosmic ray tracks.

For this measurement, the threshold for the pixels was set to a nominal value of 5000 electrons. As the gain is increased, the rate also increases to a plateau value of about 3 events per minute, which we interpret as the saturated CR rate. This rate is slightly larger than that expected from

the chip area and the total cosmic ray flux (~ 1 /cm^2/min). However, the depth of drift gap, 8.6 mm, allows CRs at moderate zenith angles to register, even if not crossing the surface of the chip. For example, at 45° a CR entering the drift gap, but directed away from the chip, can impact the plane of the pixel surface (8.6 mm)(0.707) = 6.1 mm outside the chip boundary. The measured CR plateau rate is consistent with detection of all charges on the track, single electrons as well as clusters. At this measured rate of cosmic ray events, a large sample of tracks was obtained with a threshold setting of 1800 electrons, with a gas mixture of Ar/CO_2 (70/30).

IV. Track measurements

As indicated above, we collected a large sample of CR events using the Ar/CO_2 (70/30) gas mixture, operating with an avalanche gain of approximately 9000 (GEM1/GEM2 voltages 500V/380V), and with a pixel threshold value of 1800 electrons. For most of the events, the drift field was 1.0 kV/cm, corresponding for a 1-cm drift to a transverse diffusion coefficient of 160 μm and a longitudinal coefficient of 280 μm [17].

A. Spatial resolutions

The measured point resolution is well accounted for by the hole spacing (pitch) of the GEMs, the dimensions of the pixel and the gas diffusion. The transverse diffusion in our tests, resulting from the average drift distance of 4.3 mm, is estimated to be approximately 110 μm (rms). For the ILC application, requiring much longer drift gaps, transverse diffusion will be kept relatively small by the strong magnetic field, ~ 4.0 T in current detector designs [3].

In the TPC, the Z coordinate is obtained from drift time. In our present testing arrangement, the drift space is only 8.6 mm, while in an experiment at the ILC it may be two meters or more. The timing system must be modified to record the much longer drift times. With our present pixel chip, the maximum clock speed of 40 MHz and 16 time samples correspond to a 4.0 cm drift distance at the largest drift velocities of candidate gas mixtures, about 10 cm/μs. The total drift time for 2.0 m would be 20 μs, about 50 times longer than the FEI3 time window at 40 MHz. In a specific TPC application, both the time window and clock rate would need to match specific requirements. The pixel chip, in its present form, is capable of a time resolution ~ 25 ns/$\sqrt{12}$ = 7.2 ns, and a corresponding longitudinal space resolution from timing alone, of about 720 μm at a drift velocity of 10 cm/μs.

A study was made of the track sample described above, obtained with the Ar/CO_2 gas mixture (1), and with a drift field of 1.0 kV/cm for the majority of events. All offline CR track fitting and event analyses were performed in ROOT [18]. Events were required to have at least 10 pixels above threshold (called “hits”) and the final reconstructed 3D track had to be at least 4.5 mm long. Additionally, the track-fitter disregarded any hits that contributed above a certain cutoff to the χ^2, in order to exclude extraneous hits (such as seen in Fig. 9); "CR events" included occasional pixel hits from photon-induced Compton scatters or from delta rays. The cutoff was tuned so that, for a track of average hit multiplicity, approximately 95% of hits remained assigned to the track. These cuts provided a reliable dataset for the analysis. Fig 9 shows a typical event.

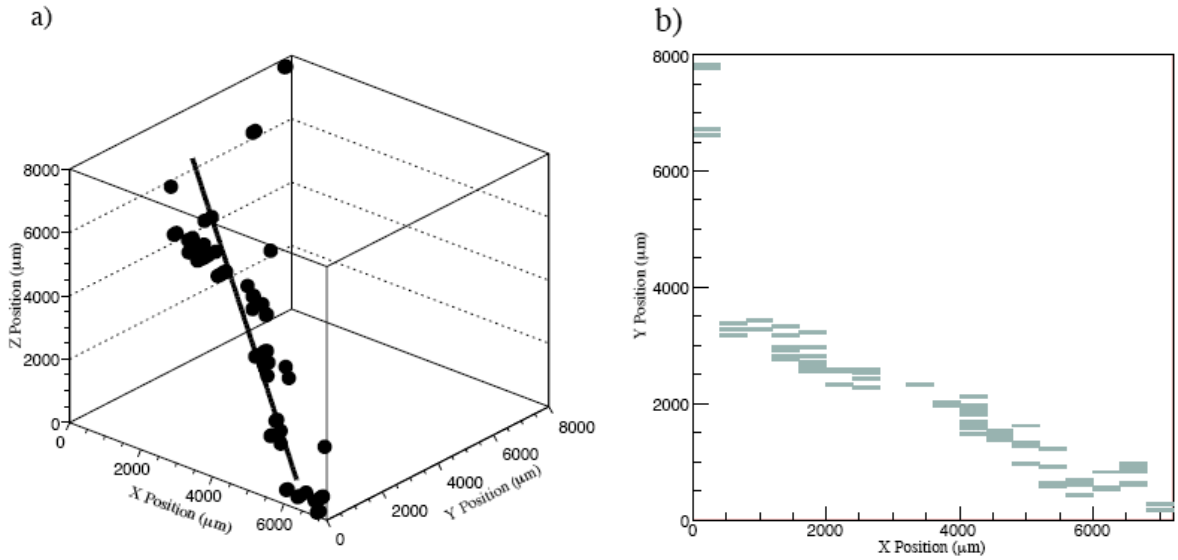

Fig. 9. A typical reconstructed event. The output is from the offline analysis software. Fig. 9(a) shows an event reconstructed in 3-D space, with points giving the centers of mass of the pixels, and the fitted track. Fig. 9(b) shows the readout of the actual pixel chip with locations of the pixel cells. Three hits far from the track were eliminated by the cut on χ^2 contribution described in the text, as not being directly associated with the track.

The 3D plot in 9(a) shows the fitted track. The X-Y space coordinates are based upon the pixel coordinates shown in Fig. 9(b), and the Z coordinates are derived from pixel timing information. The collected sample of events allowed us to measure the spatial resolution. The drift in the Z-direction during the 25-ns time bin is 650 μm, for the drift velocity of 26 μm/ns at the drift field of 1.0 kV/cm; thus the rms resolution in Z (from timing) is 190 μm, comparable to the longitudinal diffusion. From track-fitting, the measured resolutions in the X, Y and Z directions are approximately 170 μm, 130 μm and 240 μm, respectively (the X axis being parallel to the 400-μm pixel dimension). We expect that an optimized detector geometry would yield improved resolution over that measured here.

B. Using timing for cosmic ray tracks

To obtain additional confirmation of the cosmic ray source and to test the accuracy of the timing information, the dip angle of the tracks was compared to the expected $\cos^2\theta$ distribution of cosmic rays, where θ is the zenith angle (Fig. 10).

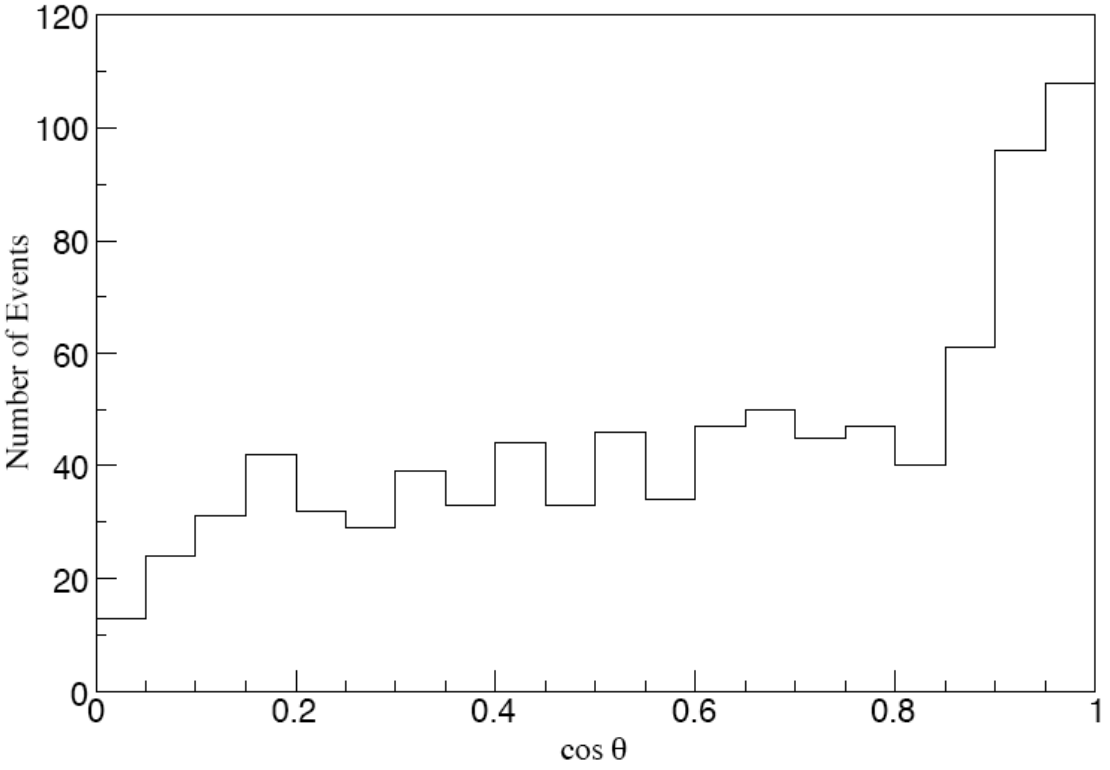

Fig. 10. The zenith angle distribution of tracks. The peak near cos θ = 1 is attributed to cosmic rays, and is peaked more strongly than $\cos^2 \theta$ because of the angular acceptance.

The distribution of tracks does show a strong peaking at small θ, but is more strongly peaked than $\cos^2\theta$. This is primarily a consequence of the geometry (drift gap vs. chip size) and corresponding acceptance. We also observe a substantial number of events at large zenith angles, possibly from low-energy Compton recoils; there are four floors of building structure above the test area that provide ample thickness for production of low-energy electron showers from cosmic ray delta rays. Scanning has revealed a few tracks (~ 6%) having very heavy local ionization deposits, probably from stopping electrons. These contribute to the angular distribution at very small values of cos θ, due to the many hits in the same time bin; and a cut requiring cos θ > 0.02 has been imposed to eliminate these.

C. Gap distribution

The distribution of hit separation, or gaps, along the tracks was also computed. The distribution of gap density (number of gaps/length) very closely follows an exponential distribution, as shown in Fig. 11.

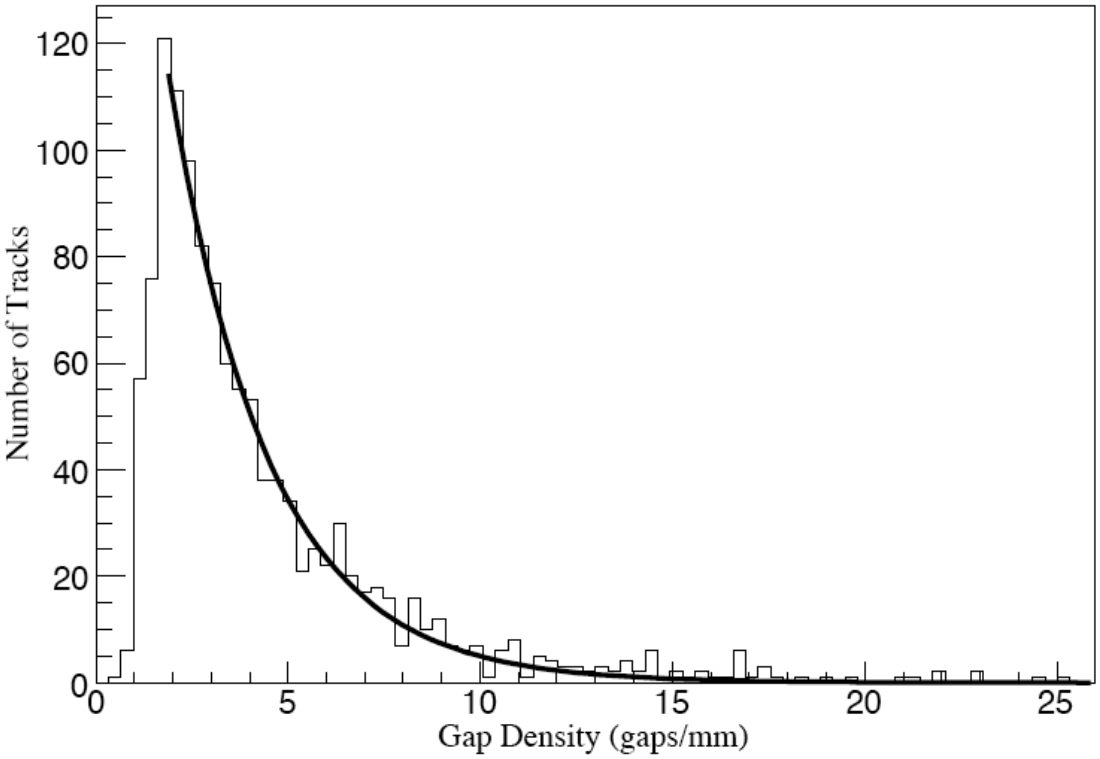

Fig. 11. Track gap density distribution. An exponential distribution provides an excellent fit to the number of gaps per mm for all tracks, with a mean gap density of 2.8 ± 0.1 per mm.

The exponential behavior is consistent with the description given by Barkas [19]. The mean gap density found from this distribution is 2.8 ± 0.10 gaps per mm, a value close to the cluster density (equivalent to gap density) given for this gas mixture by Sauli [20] and by Hauschild [21]. The avalanche gain was about 9000 for most of this collected CR sample.

D. Time-over threshold (TOT) and ionization measurements

Timing functionality in the chip allows also the measurement of charge, and therefore of ionization, for individual pixel channels. The measurement of signal pulse width above a preset discriminator threshold may be used to a good approximation as a determination of the charge on each pixel. From the collection of all pixel measurements the track ionization can be well determined.

As a confirmation of the ability of the FEI3 chip to measure simultaneously timing and ionization, the charge density along tracks has been determined using the TOT measurement, and is shown in Fig. 12.

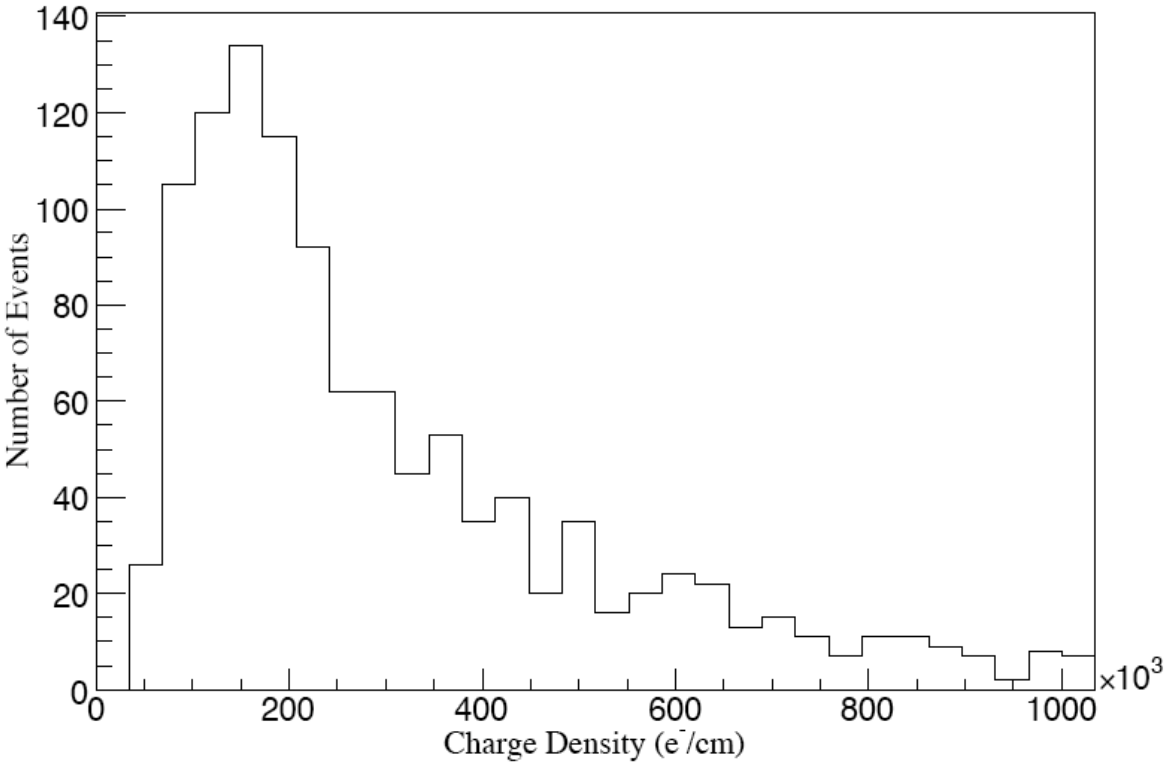

Fig. 12. Distribution of track charge density, from the time-over-threshold (TOT) measurements along tracks.

A precise determination of the primary track ionization has not been attempted, due to unknown efficiency factors (e.g., the charge not recorded when below the hit threshold). The general appearance of the expected Landau distribution is apparent, and an analysis has shown that this distribution is essentially independent of the track orientation, as expected.

V. Simulations

A. Maxwell and Garfield programs

Using the programs Maxwell [22] to perform 3D electric field calculations and Garfield [23] to study the physics of electron transport in gas mixtures, we have simulated the actual conditions of our test system with regard to diffusion and gain of drifting and avalanching electrons. Figure 13 shows an avalanche produced by a single electron drifting into the GEM avalanche region.

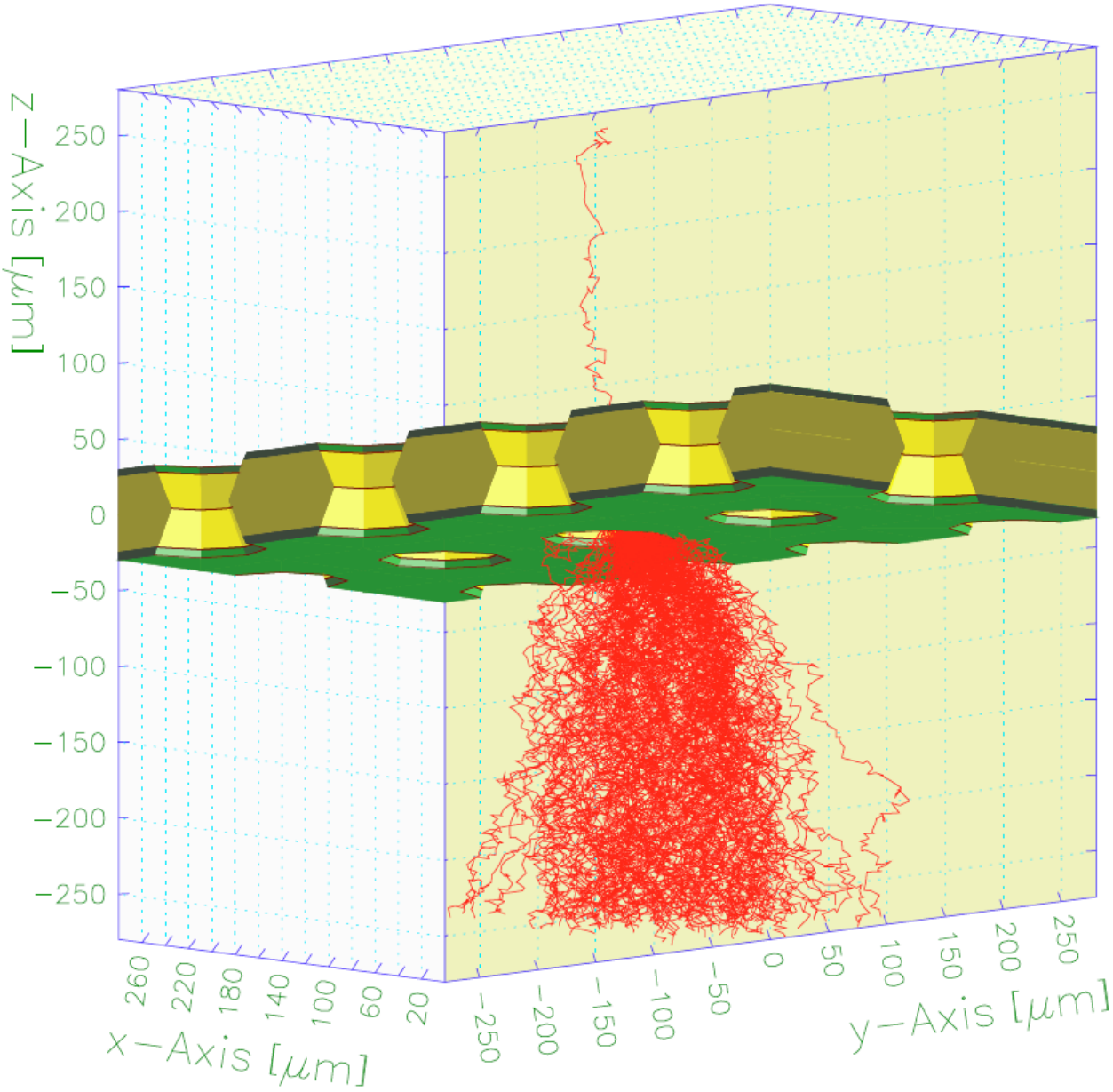

Fig. 13. A Simulated avalanche event produced by a single electron passing through a single GEM. The avalanche was created using the program Maxwell to model the electric fields generated by the GEM, and the CERN program Garfield to simulate the avalanche caused by one electron starting in the drift region. With 500 volts across the GEM, this event has a multiplication factor of 258. Only the electrons contributing to the effective avalanche gain are shown.

Under the same conditions of field strength and gas mixture, there is good agreement between the gain measured for a single GEM layer and that predicted by the simulations (but based upon a limited sample).

B. Simulation results

We have used these well-established simulation programs, Maxwell and Garfield, to examine the effects on spatial resolution of diffusion, finite GEM sampling (pitch) and electron cluster statistics. The largest effect for a TPC system at the ILC would be from the diffusion in the much

larger drift region than ours (about 2 m vs. 8.6 mm). The point resolution for our system is not a severe limitation on meeting the requirement for a TPC used in an ILC experiment, even though the present chip is not at all designed for that application (see IV. A above).

Although the intrinsic energy resolution, about 24% FWHM as recorded in the ^{55}Fe spectra, is not expected to be a limitation on track ionization measurement, it is of interest to investigate the source of this uncertainty. One contribution could be the Fano factor [24], which results from the statistical fluctuations of alternative energy flow mechanisms. In this case, the energy from the converted ^{55}Fe X-rays could result in ionization or scintillation of the excited atom, and these alternative paths can lead to large fluctuations in measured ionization charge.

Alternatively, there may be avalanche gain variations from non-uniform fields within each GEM avalanche region. As the measured gain varies approximately as $(V_{GEM})^6$, a small field variation might explain our resolution. There could also be gain variation over the active area of a GEM; the source is collimated to within ~ 6^o, resulting in an average spread of conversion electrons of about 5 mm at the upper GEM top surface, so that many avalanche holes contribute. Another possibility could be path differences between avalanche holes due to misalignment of the holes in the two GEM layers. However, for the same gain and drift field conditions, we find essentially the same resolution for a single GEM as for the double-GEM system. Recently, impressive measurements of <14% FWHM have been obtained using the Micromegas [25]. Although we have studied this question of energy resolution, we do not have sufficient information and data to resolve this issue, but consider it to be of importance and fundamental interest.

VI. Summary of tests and conclusions

We have seen that the effective avalanche gain of the double GEM is more than sufficient to produce the charge needed for nearly full efficiency in detection of track ionization, for the geometry of the FEI3 ATLAS pixel chip and for the Ar/CO_2 gas mixture (1). The maximum gain was > 40,000 before occasional discharges were noticed, but there was no damage to either the GEMs or the pixel chip. In the case of the Ar/isobutane gas mixture (2), the maximum gain obtained was about 25,000, but two discharges damaged a GEM and a chip. Further use of this gas was terminated. After replacing the GEM and chip, good operation resumed using the Ar/CO_2 mixture. Later, we tested the gas mixture (3), Ar/CH_4/CO_2 (93/5/2). This behaved very well when avalanche gains were less than about 1000, but at a larger gain the spectra were poor (subsidiary peaks); at a gain of ~ 10,000, a spark damaged both the pixel and the GEMs, and tests were terminated.

From a study of the cosmic ray (CR) event rate vs. gain, using the Ar/CO_2 mixture, and a pixel threshold setting of 5000 electrons, it was apparent that a gain of about 20,000 places the measured rate on a plateau. Under these conditions, we believe that nearly all electron clusters and single electrons are detected with high efficiency on minimum-ionizing tracks. This is confirmed both from the asymptotic shape of the plateau curve (Fig. 8) and from a comparison of the threshold and effective gain settings. For the purpose of track detection (and not to demonstrate the saturation of the cosmic ray rate), the threshold could be set lower, about 2000 to 3000, and the avalanche gain adjusted appropriately. A specific design for ILC use may have a smaller pixel area, allowing a much lower threshold.

Spectra using an ^{55}Fe source with gas (1) yielded an energy (or charge) resolution of about 24% FWHM for the principal peak at 5.9 keV. The general appearance of the spectra was very good for all three gas mixtures tested, allowing accurate determinations of the effective avalanche

gain. However, the energy resolution is not of any special importance to the TPC readout, since the average of charge measurements, pixel-by-pixel, over a track length, or, alternatively, cluster counting, which is independent of charge resolution, can give accurate determinations of ionization density for particle identification.

A large sample of tracks was obtained with use of the Ar/CO_2 gas mixture and a pixel threshold of 1800 electrons. An analysis was done of the point spread of pixel hits for those tracks selected as good candidates for such measurements: long and straight tracks with small ionization (few hits per length). The transverse and longitudinal resolutions were measured, giving values of approximately 170 μm, 130 μm and 240 μm, for the X, Y and Z directions, respectively. In a full- scale TPC readout of tracks 50 cm or more, the resolution required for the ILC would be met, assuming that the present readout system could be scaled up without loss of precision. Because the FEI3 chip was designed for a completely different application, an optimization for the TPC at the ILC is required. The size, shape and pitch of the pixels will be different, and the timing buffer must be greatly extended to accommodate drift distances of ≥ 2.0 meters.

Certain possible detector problems have not been addressed in the investigations reported here. One is the backflow of positive ions from the GEM avalanches. A limited positive charge can enter the drift volume before the resulting perturbation of the drift field seriously distorts the track. Gating techniques have been proposed, perhaps requiring another electrode layer [26]. A potential risk is that of electrical discharge or sparking, to which the chips are especially vulnerable. A single spark to the chip, or even in the vicinity of the chip, could destroy it. All measurements using the Ar/CO_2 were accomplished with no damaging discharges, over a long period of testing, but we did have breakdown problems and damage with both the Ar/isobutane and the Ar/methane/CO_2 gas mixtures. Moreover, sparking can be easily induced by heavily ionizing particles that may be encountered in a full-scale accelerator experiment, although not encountered in laboratory tests.

Although measurements have been done using the Micromegas as the avalanche device, these studies have not been fully pursued. Other groups have been actively pursuing similar TPC readout techniques, especially the groups of Timmermans, Bamberger, Colas and Bellazzini [27].

Acknowledgments

We wish to thank several people for their contributions to this project: Marco Battaglia for suggesting it, Maurice Garcia-Sciveres for supplying the FEI3 chips, Craig Tindall for post-processing these chip, and George Zizka for designing a new custom PC board for our application as well as guiding much of the fabrication. We appreciate the assistance, advice and interest from Fabio Sauli in the development of this project. We have benefited from discussions with David Nygren and Richard Kadel. We also are indebted to Rob Veenhof (CERN) for his help with the Garfield program. We thank also Richard Kuiper, Rodolfo Bartolo and Thomas Weber for their parts in the mechanical construction.

This work was supported by the Director, Office of Science, Office of High Energy Physics, of the U.S. Department of Energy under Contract No. DE-AC02-05CH11231.

References

[1] D. R. Nygren, A Time Projection Chamber, Proceedings of the 1975 PEP Summer Study, LBL Berkeley, 1975; J. Marx, D. Nygren, The Time Projection Chamber, Phys. Today, Oct. 1978.

[2] G. Charpak, D. Rahm, H. Steiner, Nucl. Inst. and Meth. 80 (1970) 13.

[3] ILC Reference Design Report, August 2007, http://www.linearcollider.org/cms/?pid=1000437, Volume 4 - Detectors, Section 5.3 GASEOUS TRACKING

[4] F. Sauli, Nucl. Instr. and Meth. A 386 (1997) 531.

[5] Y. Giomataris, et al., Nucl. Instr. and Meth. A 376 (1996) 29.

[6] I. Peric, et al., Nucl. Instr. and Meth. A 565 (2006) 178.

[7] The specification in the CERN stores catalog is: GEM-50x50-140-70/50-P-F (catalog no. 08.82.00.051.7), CERN, Meyrin, Switzerland.

[8] MAESTRO-32 MCA Emulator, ORTEC, Oak Ridge, TN.

[9] A. Peisert, F. Sauli, Drift and diffusion of electrons in gases: a compilation, CERN 84-08, Experimental Physics Division, July 1984. F. Sauli, private communication.

[10] MOD. N 470 4-channel (programmable) HV Power Supply, CAEN, Staten Island, NY 10302.

[11] Model eV-5093 preamplifier, eV Products, Saxonburg, PA.

[12] TranLamp: A shaper amplifier developed at LBL for the Nuclear Science Division, designed by B. Kaifer, G. Kilian, B. Larsh, D. Mosier and W. Goldsworthy, 1964. Print no. 15X4845.

[13] C. Meroni, Nucl. Instr. and Meth. A 572 (2007) 92.

[14] TurboDAQ, LBNL ATLAS Group, Berkeley, http://pixdata.lbl.gov/html/TurboDAQ.htm.

[15] R. Bellazzini, et al., A new VLSI counting chip for micropattern gas detectors, IEEE Nuclear Science Symposium, Hawaii, October 2007, http://www.nss-mic.org/2007/program/listprogram.asp?session=n12.

[16] M. Hamann, R&D for the GEM readout of the TESLA TPC at DESY/University of Hamburg, International Workshop on Linear Colliders, Jeju Island, Korea, August 2002 http://lcws2002.korea.ac.kr/ (Programs, Parallel Session G. Tracking, Tues. AM, 27 Aug.) and http://arxiv.org/abs/hep-ex/0301006; M. Kobayashi et al., Nucl. Instr. and Meth. A 581 (2007) 265.

[17] Same as reference [9], p 30 (σ_T) and p 39 (σ_L). The plot for σ_L is for the mixture Ar/CO_2 (80/20), but is expected to be similar for the Ar/CO_2 (70/30) mixture.

[18] R. Brun, F. Rademakers, Nucl. Instr. and Meth. A 389 (1997) 81.

[19] W. Barkas, Phys. Rev. 124 (1961) 897.

[20] F. Sauli, CERN 77-09, 3 May 1977. The values per cm given for Ar and CO_2 are 29.4 and 34, respectively, yielding 31 clusters/cm for this mixture.

[21] M. Hauschild, International Workshop on Linear Colliders, Jeju Island, Korea, August 2002 http://lcws2002.korea.ac.kr/ (Programs, Parallel Session G. Tracking, Tues. PM, 27 Aug.), where the value given is 20-30 clusters/cm, in good agreement with our result. See also M. Hauschild talk, TPC ILC Workshop, DESY, 13 Feb. 2006, http://ilcagenda.linearcollider.org/conferenceDisplay.py?confId=desya0591.

[22] Maxwell 3D, Ansoft, Pittsburg, PA, http://www.ansoft.com/products/em/max3d.

[23] R. Veenhof, Nucl. Instr. and Meth. A 419 (1998) 726.

[24] U. Fano, Phys. Rev. 72 (1947) 26.

[25] J. Timmermans, ALCPG2007 (Amer. Linear Collider Physics Grp.) – FNAL, 23 Oct. 2007, http://ilcagenda.linearcollider.org/contributionDisplay.py?contribId=141&sessionId=10&confId=1556.

[26] F. Sauli, L. Ropelewski, P. Everaerts, Nucl. Instr. and Meth. A 560 (2006) 269.

[27] J.L. Visschers et al., Nucl. Instr. and Meth. A 572 (2007) 203; A. Bamberger et al., Nucl. Instr. and Meth. A 573 (2007) 361 and A581 (2007) 274; R. Bellazzini et al., Nucl. Instr. and Meth. A 581 (2007) 246; V.M. Blanco Carballo et al., Nucl. Instr. and Meth. A 583 (2007) 42.